A Transformed Symmetrical Condensed Node for the Effective TLM Analysis of Guided Wave Problems

Malgorzata Celuch-Marcysiak and Wojciech K. Gwarek, *Senior Member, IEEE*

***Abstract*—We propose a novel TLM algorithm for the effective solution of arbitrary guided wave problems. The algorithm uses an appropriately transformed symmetrical condensed node introduced herein. In comparison with the previous SCN TLM formulation for the analysis of guiding structures, our approach maintains equivalent accuracy and generality while providing a 50% gain in terms of required computer memory and time. The advantages of our algorithm are verified by means of several examples, including full - wave analysis of waveguides filled with anisotropic and lossy media.**

I. Introduction

In the microwave frequency range of crucial importance is the ability to accurately and efficiently solve guided wave problems. Dispersion characteristics as well as field distribution of various modes in a guiding structure have to be known for proper designing of a microwave circuit. Since a plethora of microwave guiding structures are currently in use, a versatile analysis algorithm should be capable of modelling waveguides with arbitrarily shaped cross-sections and filled with inhomogeneous and anisotropic media. Such capabilities are inherent in the time-domain methods [1]. However, a direct 3-D time-domain approach to guided wave problems as proposed in [3] is not attractive for a designer due to extensive computer memory and time requirements.

To obviate this efficiency problem we have to note that if the propagation along the guide proceeds with a particular phase constant β, the analytical description of fields in the direction of propagation is known and the numerical analysis can be reduced to the guide's cross-section. So far, three algorithms based on this approach have been proposed:

1. a specialized version of the 2-D FD-TD method [2],
2. a TLM algorithm using a symmetrical condensed node (SCN) and complex notation in the time domain [4], [5],
3. an FD-TD algorithm using complex notation [6].

In this contribution we propose an alternative formulation based on the appropriately transformed SCN. In terms of accuracy and generality, our algorithm is fully equivalent to the method of [4], but it provides an over 50% gain in both computer memory and time required to solve any particular problem.

Manuscript received July 6, 1992; revised September 23, 1992.
M. Celuch-Marcysiak is with Institute of Radioelectronics, Warsaw University of Technology, Nowowiejski 15/19, 00-665 Warsaw, Poland.
W. K. Gwarek is with Franco-Polish School of New Information and Communication Technologies, Mansfelda 4, 60-854 Poznan, Poland.
IEEE Log Number 9207417.

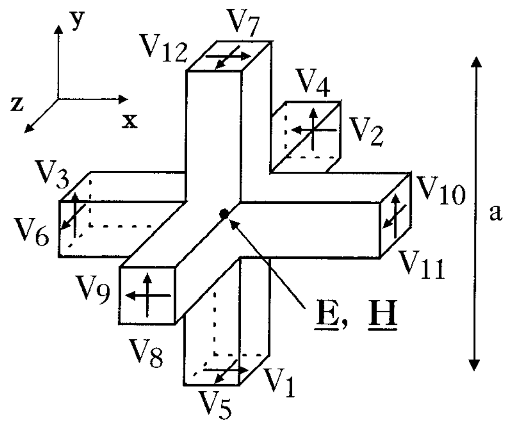

Fig. 1. Symmetrical Condensed Node after Johns [7].

II. A Transformed Symmetrical Condensed Node

A fundamental structure of the SCN after [7] is shown in Fig. 1. Inhomogeneous and anisotropic media are modelled by additional six stubs 13..18 at the node. Scattering at the node is described by an 18×18 matrix S [7].

The complex SCN TLM algorithm of [4] follows from closing the arms of the node along the direction of propagation by a nonreciprocal phase shift:

$$\begin{aligned} {}^iV_{11}^{k+1} &= {}^rV_3^k \exp(j\beta a) \\ {}^iV_{10}^{k+1} &= {}^rV_6^k \exp(j\beta a) \\ {}^iV_3^{k+1} &= {}^rV_{11}^k \exp(-j\beta a) \\ {}^iV_6^{k+1} &= {}^rV_{10}^k \exp(-j\beta a) \end{aligned} \quad (1)$$

where β is the propagation constant along the guide, a is the space discretization step, prescripts indicate incident and reflected quantities, superscripts—time instants and subscripts—line numbers according to Fig. 1. This approach permits to eliminate one space dimension from the analysis, in exchange however for introducing the complex numbers.

Let us propose the following transformation of the SCN. Instead of pulses on lines 3, 6, 10, 11 (Fig. 1) we consider their linear combinations:

$$\begin{aligned} \underline{V}_3 &= V_3 + V_{11} \qquad & \underline{V}_{11} &= V_{11} - V_3 \\ \underline{V}_6 &= V_6 + V_{10} \qquad & \underline{V}_{10} &= V_{10} - V_6 \end{aligned} \quad (2)$$

In the result we observe that:

a) at each node, the scattering matrix S assumes a block-diagonal form, so that instead of one 18×18 scattering equation we deal with two 9×9 scattering equations, —

one equation involves only pulses on branches $\{B1\} = \{1, 2, 9, 12, \underline{10}, \underline{11}, 13, 17, 18\}$ where 13,17,18 are nodal stubs (not included in Fig. 1) which account for inhomogeneous ϵ_x, μ_y, μ_z, respectively; —the other equation involves pulses on branches $\{B2\} = \{4, 5, 7, 8, \underline{3}, \underline{6}, 14, 15, 16\}$ where 14,15,16 are stubs which account for $\epsilon_y, \epsilon_z, \mu_x$,

To explain this separation let us note that none of the classical SCN branches $\{1, 2, 9, 12\}$ is directly coupled to $\{4, 5, 7, 8\}$. Furthermore, the newly defined branches $\underline{3}, \underline{6}$ are separated from $\{1, 2, 9, 12\}$ and $\underline{10}, \underline{11}$ are separated from $\{4, 5, 7, 8\}$. The only direct coupling between $\{B1\}$ and $\{B2\}$ proceeds through $\underline{3}$ coupled to $\underline{11}$ and $\underline{6}$ coupled to $\underline{10}$.

b) in place of the coupling equations (1) we obtain for example for line $\underline{3}$:

$$\begin{aligned} {}^{i}\underline{V}_3^{k+1} &= {}^{i}V_3^{k+1} + {}^{i}V_{11}^{k+1} \\ &= {}^{r}V_{11}^{k} \exp(-j\beta a) + {}^{r}V_3^{k} \exp(j\beta a) \\ &= \left[{}^{r}V_3^{k} + {}^{r}V_{11}^{k}\right] \cos(\beta a) + j\left[{}^{r}V_3^{k} - {}^{r}V_{11}^{k}\right] \sin(\beta a) \\ &= {}^{r}\underline{V}_3^{k} \cos(\beta a) - j{}^{r}\underline{V}_{11}^{k} \sin(\beta a) \end{aligned} \tag{3}$$

c) in view of the form of equation (3) we note that our algorithm can be operated with all pulses on branches $\{B1\}$ being purely real: $V = U$, and all pulses on $\{B2\}$—purely imaginary: $V = jW$ (while in [4], to be able to satisfy equations (1), pulses on all branches had to be admitted complex values);

d) eventually, the coupling equations for lines perpendicular to the guide's cross-section take the form:

$$\begin{aligned} {}^{i}\underline{W}_3^{k+1} &= {}^{r}\underline{W}_3^{k} \cos(\beta a) + {}^{r}\underline{U}_{11}^{k} \sin(\beta a) \\ {}^{i}\underline{U}_{11}^{k+1} &= -{}^{r}\underline{U}_{11}^{k} \cos(\beta a) + {}^{r}\underline{W}_3^{k} \sin(\beta a) \\ {}^{i}\underline{W}_6^{k+1} &= {}^{r}\underline{W}_6^{k} \cos(\beta a) + {}^{r}\underline{U}_{10}^{k} \sin(\beta a) \\ {}^{i}\underline{U}_{10}^{k+1} &= -{}^{r}\underline{U}_{10}^{k} \cos(\beta a) + {}^{r}\underline{W}_6^{k} \sin(\beta a) \end{aligned} \tag{4}$$

Consequently, with no loss of accuracy or generality we have reduced the complex algorithm of [4] to real number calculations, with half of the memory cells and less than half of the operations needed for [4].

In Fig. 2 we present a structure of the transformed node. This structure leads to an interesting physical interpretation of the proposed numerical scheme. Essentially, the transformed node is composed of two sub-nodes which represent solutions of two 2-D scalar problems, concerning two modes of a planar circuit (the guide's cross-section). The two modes are:

1. TM mode (with respect to the axis of the guide, i.e. the x-axis in Fig. 2)—comprising the E_x, H_y, H_z field components,
2. TE mode—comprising the H_x, E_y, E_z field components.

A link between the two sub-nodes provides the coupling of the two scalar solutions above the cutoff frequency of the guiding structure, through the transversal field components E_y, E_z, H_y, H_z.

It must be noted that excitation through one of the modes produces the other mode with the spatial phase shift of $\pi/2$ corresponding to the physical conditions of a standing wave.

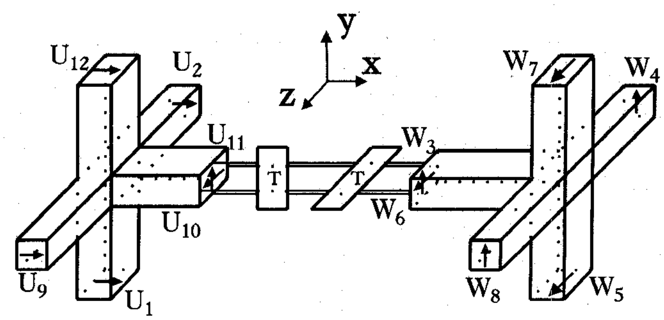

Fig. 2. Transformed Symmetrical Condensed Node introduced herein.

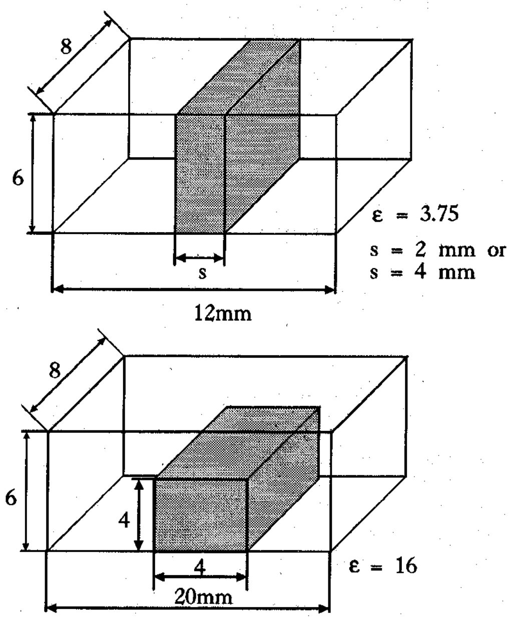

Fig. 3. Inhomogeneous LSE—mode and hybrid—mode resonantors.

In the complex notation of [4] it is possible to consider a travelling wave but numerically it corresponds to the combination of two separately analyzed standing waves. This explains why the complex notation of [4] requires more computer effort.

III. Examples of Calculations

We analyzed the inhomogeneous resonators with cross-sections invariant in one direction, as in Fig. 3. In terms of dispersion characteristics of waveguides with the same cross-section, such calculations correspond to obtaining a series of frequencies at which consecutive modes propagate with the assumed phase constant.

In Table I we present the fundamental resonant frequencies obtained with the transverse resonance method [3], the 3-D FD-TD method [3] and our method. If the same mesh size is used for the direct 3-D approach and our 2-D approach, the 2-D results appear closer to the transverse resonance reference. This is a direct consequence of a lower level of numerical dispersion in a 2-D model as compared to 3-D [8].

We then calculated the dispersion characteristics of a shielded microstrip after [3]. While at low frequencies our results coincide with those of the direct 3-D FD-TD approach,

TABLE I

resonator	TRM	3-D FD-TD a = 1mm	transf. SCN a = 1mm	transf.SCN a = 0.5mm
Fig.3a s = 2mm	15.66	15.51	15.62	15.64
Fig.3a s = 4mm	13.35	13.26	13.33	13.35
Fig.3b	—	8.34	8.34	8.40

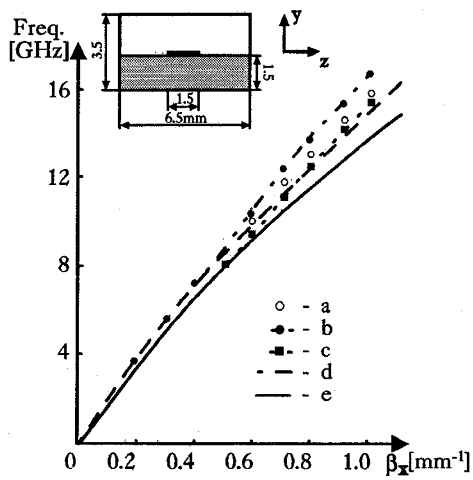

Fig. 4. Dispersion characteristics of a shielded microstrip on isotropic ($\epsilon_r = 9.4$) and anisotropic ($\epsilon_x = \epsilon_z = 9.4, \epsilon_y = 11.6$) dielectric: (a) isotropic, transformed SCN, $a = 0.5$ mm; (b) isotropic, transformed SCN, $a = 0.25$ mm; (c) anisotropic, transformed SCN, $a = 0.25$ mm; (d) isotropic, 3-D FD-FD, $a = 0.5$ mm [3]; (e) anisotropic, 3-D FD-TD, $a = 0.5$ mm [3].

some discrepancy is observed at higher frequencies (Fig. 4). This is again a consequence of smaller numerical dispersion for the 2-D model. As a reference, calculations with the refined space discretization can serve.

To demonstrate the ability of our algorithm to analyze anisotropic media we further considered the same microstrip structure, but on the anisotropic substrate. The results are included in Fig. 4.

Finally, we have extended the transformed SCN TLM algorithm to lossy media. It must be noted that neither this algorithm nor the complex SCN TLM [4], [5] allow for direct incorporation of complex wave numbers since these would cause instability of calculations. Therefore, in both our method and [5] losses are considered indirectly, by means of a quality factor of a resonator. Our procedure comprises the following steps:

1. Neglecting losses, we compute the dispersion characteristics $\beta = \beta(\omega)$.
2. We assume that losses are small enough not to modify significantly the dispersion characteristics $\beta = \beta(\omega)$, so that only the characteristic of $\alpha = \alpha(\omega)$ remains to be determined.
3. For each ω, we excite the structure by a sinusoidal source. Integrating the energy stored within the structure W and the power dissipated per period $Po\frac{1}{f}$ we obtain the quality factor of the resonator Q.

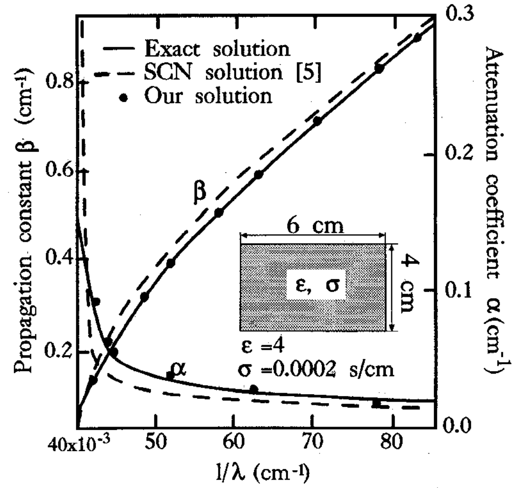

Fig. 5. Dispersion characteristics of a rectangular waveguide filled with a lossy dielectric.

4. We calculate the attenuation constant α as:

$$\alpha = \frac{1}{2Q}\omega\frac{\partial\beta}{\partial\omega} \tag{5}$$

with $\frac{\partial\beta}{\partial\omega}$ deduced from the inclination of curve $\beta = \beta(\omega)$ is obtained in Step 1.

In Fig. 5 we compare our solutions, analytical solutions and the solutions of [5] for a rectangular waveguide filled with a lossy dielectric [5]. As expected for small losses, the agreement of our approach with theory is very good.

Fig. 5 also reveals a relative advantage of our results as contrasted to the results of [5]. We presume that this advantage resides in our implementing of a more accurate model of excitation, as discussed in [9]. Excitation classically used for the time-domain analysis of eigenvalue problems consists in directly setting initial field values within a circuit. After reaching the steady state, eigenfrequencies are determined as maxima of the Fourier transform of selected field components, at selected locations [3]. The new form of exictation [9] incorporates a pulse source modelled by an equivalent scheme including finite resistance. Eigenfrequencies are determined as minima of the Fourier transform of the current injected to the circuit by the source. For frequencies different from the resonance, energy is dissipated in the source resistance. Consequently, the minima are sharper, obtained with better resolution and after a smaller number of iterations than the maxima in the classical approach.

IV. Conclusions

We have introduced a new 2-D SCN TLM algorithm for analyzing arbitrary guiding structures. When compared with the previous 2-D SCN TLM approach proposed in [4], this algorithm produces indistinguishable results for all examined types of circuits, provided that equivalent models of excitation are used in both cases. Simultaneously, our formulation gives an over 50% gain in both computer time and memory and leads to a valuable physical interpretation.

In comparison with the direct 3-D approach, the presented algorithm provides a gain in efficiency by at least an order of magnitude. Additionally, it proves more accurate as a result of smaller numerical dispersion of the 2-D models.

Observed differences between the transformed SCN TLM and the FD-TD formulation of [2] are indeed a direct consequence of the two algorithms being based on two distinct models of the electromagnetic space: the condensed node and the Yee's mesh, respectively. In detail, we have examined the differences between these two models of space in [8]. General conclusion is that for a particular mesh size, the algorithm based on the (transformed) SCN introduces smaller dispersion within homogeneous regions, at the expense of greater requirements of computer memory and time.

Throughout the paper, we have not related the transformed SCN TLM to the complex FD-TD of [6]. Instead we have checked that the complex FD-TD of [6] provides equivalent results as the FD-TD formulation of [2]. In other words, the relationship between the complex FD-TD of [6] and the FD-TD of [2] is analogous to that between the complex SCN TLM of [4] and the transformed SCN TLM of this paper.

REFERENCES

[1] W. Gwarek, "Analysis of arbitrarily - shaped two dimensional microwave circuits by finite - difference time - domain method," *IEEE Trans. Microwave Theory Tech.*, vol. 36, pp. 738–744, no. 4, April 1988.
[2] C. Mroczkowski and W. Gwarek, "Microwave circuits described by two-dimensional vector wave equation and their analysis by FD-TD method," *XXI Eur. Microwave Conf.*, Stuttgart 1991, pp. 199–204.
[3] D. H. Choi, W. J. R. Hoefer, "The finite - difference time- domain method and its application to eigenvalue problems," *IEEE Trans. Microwave Theory Tech.*, vol. MTT-34, pp. 1464–1470, no. 12, Dec. 1986.
[4] H. Jin, R. Vahldieck, and S. Xiao, "An improved TLM full - wave analysis using a two dimensional mesh," *IEEE MTT Symp. Dig.*, Boston 1991, pp. 675–678.
[5] H. Jin, R. Vahldieck, and S. Xiao, "A full - wave analysis of arbitrary guiding structures using a two - dimensional TLM mesh," *XXI Eur. Microwave Conf.*, Stuttgart 1991, pp. 205–210.
[6] S. Xiao, R. Vahldieck, and H. Jin, "Full-wave analysis of guided wave structures using a novel 2-D FD-TD," *IEEE Microwave Guided Wave Lett.*, vol. 2, pp. 165–167, no. 5, May 1992.
[7] P. B. Johns, "A symmetrical condensed node for the TLM method," *IEEE Trans. Microwave Theory Tech.*, vol. MTT-35, pp. 370–377, no. 4, Apr. 1987.
[8] M. Celuch-Marcysiak and W. Gwarek, "On the aspects of selecting the symmetrical condensed node or the expanded node modelling for electromagnetic simulations," *XXII Eur. Microwave Conf.*, Helsinki Aug. 1992, pp. 350–355.
[9] W. Gwarek, "On the proper choice of excitation in the analysis of electromagnetic eigenvalue problems by finite-difference time-domain method," *Eur. Conf. on Numerical Methods in Electromagnetism, " Numelec'92"*, Grenoble, March 1992.

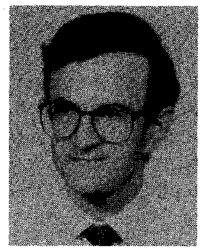

Wojciech K. Gwarek (SM'90) was born in Poland. He received the M.Sc. (1974) from Massachusetts Institute of Technology, Ph.D. (1977) and Habilitation (1988) from the Warsaw University of Technology, Warsaw, Poland. He is currently Professor of Franco-Polish School of New Information and Communication Technologies in Poznan, Poland and Associate Professor of the Warsaw University of Technology.

During the academic year 1991/1992 he was a visiting professor at Ecole Nationale Superieure de Telecommunications de Bretagne, Brest, France. He is author of many scientific papers, a text-book on electromagnetic theory and a software package named Quick-Wave (distributed by ArguMens GmbH, Duisburg, Germany). His research interests are in the areas of electromagnetic field theory and computer-aided analysis and design of microwave circuits. Dr. Gwarek is a member of Editorial Board of IEEE Transactions on Microwave Theory and Techniques and a Member of the Technical Programme Committee of the European Microwave Conference.

Malgorzata Celuch-Marcysiak was born in Warsaw, Poland, in 1964. She is a graduate of the United World Colleges. In 1988 she received the M.Sc. degree (honors) in electronic engineering from the Warsaw University of Technology. Currently she is working towards the Ph.D. degree at the Institute of Radioelectronics, Warsaw University of Technology.

Her research interests are in the area of electromagnetic field theory and numerical analysis of microwave circuits, with particular emphasis on relationships between various numerical methods.